Jurnal Rekayasa Elektrika Vol. 20, No. 4, December 2024, page 134-142

ISSN. 1412-4785; e-ISSN. 2252-620X, Accredited by Kemendikbudristek No. 105/E/KPT/2022
DOI: 10.17529/jre.v20i4.37537

Optimization of Electrospinning Temperature Control System IoT-Based with DHT21

Della Astri Widayani, Luluk Arifatul Hikamiah, Panji Setyo Nugroho, Dewa Pascal Ariyanto, Jasmine Cupid Amaratirta, Dewanto Harjunowibowo, and Yulianto Agung Rezeki*
Departement of Physics Education, Universitas Sebelas Maret
Jl. Ir. Sutami 36, Surakarta, 57126
*e-mail: yarezeki@staff.uns.ac.id

Abstract—**Electrospinning is a method of making nanomaterials that has a fairly easy and flexible process that can produce nanofiber continuously. Nanofiber morphology from the electrospinning process is influenced by several parameters, one of them is temperature as an environmental parameter. If there is no temperature control system in the electrospinning system, it will be difficult to maintain the consistency of the morphology nanofiber and at certain temperatures, nanofibers are not formed. Therefore, this study aims to develop a temperature control system for electrospinning called the electrospinning temperature control (ETC) system and connect it with an internet-of-things (IoT) platform to understand the dynamics of the temperature control process, upload temperature data to the cloud, and remote monitoring. The method used by designing and building system hardware and software, calibrating DHT21 as a temperature sensor and testing system performance. The results show that the calibration of the DHT21 sensor has an accuracy rate of 94.95% and a precision rate of 98.93%, while the results of the performance test show that the system can raise, maintain, and lower the temperature. Further performance testing reveals that the ETC system can operate within a temperature range of 20−40°C. The IoT system using the Blynk App allows users to remote and monitor easily, and using Google Sheets as a cloud database. The ETC system was successfully built and can be applied to electrospinning experiments.**

Keywords: ***blynk app, DHT21, electrospinning temperature control, ESP8266, nodemcu***

I. Introduction

Nanotechnology holds immense potential to revolutionize human life by pushing the frontiers of technology across diverse fields. This includes applications in chemistry for investigating carbon structures at the nanoscale, in computer science where nanotechnology contributes to increasingly compact computer designs for information storage, in biology for innovative bio-cell manipulation through nanostructures, and in physics as a technique for characterizing materials and evaluating the properties of nanomaterials [1]. Nanomaterials have nanometer sizes ranging from 1−100 nm, thus nanomaterials have superior structures and are effective for their application or use in various fields [2]–[4]. One method of nanomaterials production is electrospinning, a fairly easy and flexible process that can continuously produce nanomaterials [5], [6].

The temperature during the electrospinning process should be kept stable. Significant temperature changes can affect the flow of solution through the spinneret and the formation of the resulting materials [7]–[10] research groups around the globe are focusing more on the preparation of nanomaterials for various applications. Among the various techniques reported in the literature, electrospinning has gathered significant interest because of its ability to fabricate nanostructures with unique properties such as a high surface area and inter/intra fibrous porosity. Electrospinning has been the most widely used technique in the late 20th (1990). In 2017, Yang et al. said that increased temperature during electrospinning can accelerate solvent evaporation [11]. Each polymer solution requires specific temperature settings to optimize nanofiber production, ensuring structures without beads and consistent fiber diameters. Huang et al. [12] used a PVDF solution and showed that beads were nearly nonexistent within the temperature range of 25−35°C. Hardick et al. in 2011[13], stated that 25°C is the optimal temperature for producing cellulose acetate nanofibers with high diameter uniformity. In 2020, Thuy et al. [14] indicated that uniform chitosan nanofibers could be obtained at solution and chamber temperatures of 32°C. These studies showed that the optimal temperature is in the range of 25−35°C. Although it may still be possible to perform electrospinning without a temperature controller, if a temperature control system is in place, the consistency and finish of the nanofibers produced will be better maintained. Therefore, a temperature control device is needed to control the temperature in the electrospinning system to keep it stable.

In previous studies, Chen & Yu in 2010 [15] made temperature control for electrospinning by wrapping the syringe pump with a heater film, then Lara-Padilla et al. in 2017 made a cooling system using Peltier thermopiles [16]. Besides that, Thuy et al. [14] also made temperature control

Received 23 February 2024; Revised 28 November 2024; Accepted 30 November 2024

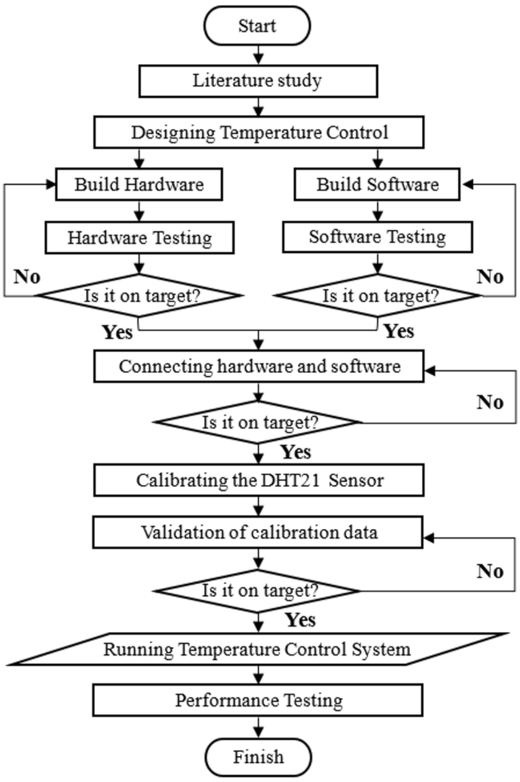

Figure 1. Research methodology

using a coil surrounding the syringe pump and installed electric heaters on both sides of the electrospinning room. Further, Abbas et al. [17] made a syringe pump jacket that was connected to a commercial thermostatic bath Then, in the following year, Lv et al. in [18] diameter, crystallinity, thickness, and mechanical characteristics. The experimental results showed that the combined effect of two parameters, the temperature of the receiver plate and the magnetic field generated by the magnetic lens let to the production of fibers with a smaller diameter (308 nm) made temperature control using a silicone rubber heating plate placed behind the collector plate. These researches mostly focus on heating the solution, while there is limited research on adjusting the room temperature, and remote monitoring and controlling Internet-of-Things (IoT)-based has never been applied. Therefore, this study aims to develop a temperature control for electrospinning called electrospinning temperature control (ETC) system by adjusting the room temperature to regulate the solvent evaporation rate. Regarding temperature sensors, the ETC system uses DHT21 because this sensor has high precision and is resistant to corrosion [19]. The ETC system is connected to the IoT platform to learn the dynamics of the temperature control process, export temperature data to the cloud, also remote and monitor easily.

II. Method

A. Research Design

In this work, an experimental method is used which includes design, assembly, data collection, sensor calibration, and testing, as shown in Figure 1. The design begins with a literature study also designing hardware and software, then assembling all components according to the schematic, then uploading the code in the Arduino IDE and creating software such as Blynk and Google Sheets applications, and data collecting was carried out for DHT21 sensor calibration and testing system performance.

Table 1. ETC system components

No.	Compo-nents	Function
Hardware		
1.	NodeMCU	NodeMCU is equipped with an ESP8266 chip and features digital and analog I/O pins to connect various sensors and actuators. This module has Wi-Fi integrated capabilities, allowing the device to communicate with other devices wirelessly [20].
2.	Relay 2 channel	Relay 2 channels as a switch to regulate heat components and cold components.
3.	Heat component	The heat component is a nichrome wire mounted on a PCB plate, connected to a positive cable and a negative cable so that it functions to generate heat.
4.	Cold component	The cold component is a Peltier connected with the heatsink and coldsink, where the heatsink is used to remove heat from the Peltier, and the cold sink is used to accommodate the cold from the Peltier.
5.	Power supply	Power supply is used to supply power that can supply 12 volt 10 Ampere.
6.	DHT21	DHT21 or AM2301 is a temperature and humidity sensor. This sensor can precisely provide environmental temperature data and is susceptible to corrosion [21].
7.	DC fan	The DC fan is a wind-producing device used in this project to carry wind through heat and cold components.
8.	4×4 matrix keypad	A keypad is a series of buttons used in this project to enter the desired temperature.
9.	LCD I2C	The LCD is used to display temperature information.
Software		
1.	Blynk App	Blynk App can create mobile apps that connect with hardware such as microcontrollers, sensors, and actuators and control them through the internet network [22].
2.	Arduino IDE	The Arduino IDE supports the C/C++ programming language, a common language used in hardware development [23].
3.	Google sheets	Google Sheets is a cloud application in the form of tables used to process data, store data, create graphs, etc. This application can be shared by many people [24].

B. Design Temperature Control

The design begins with a literature component, circuit, system, and controller design. The ETC system components consist of hardware and software, as shown in Table 1.

The circuit design is achieved by synthesizing software,

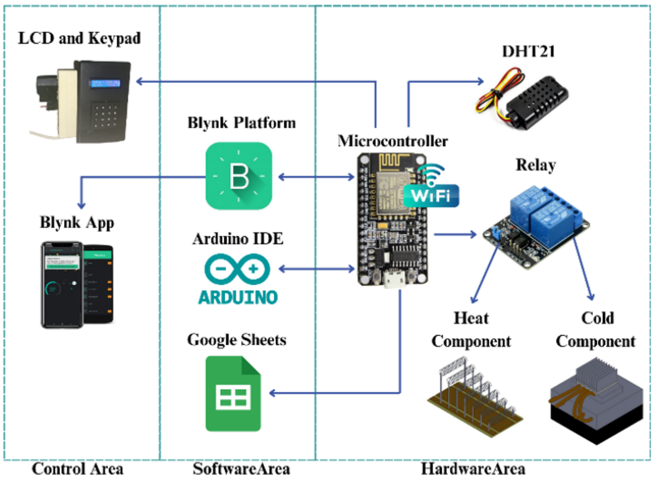

Figure 2. Schematic showing the connection between components

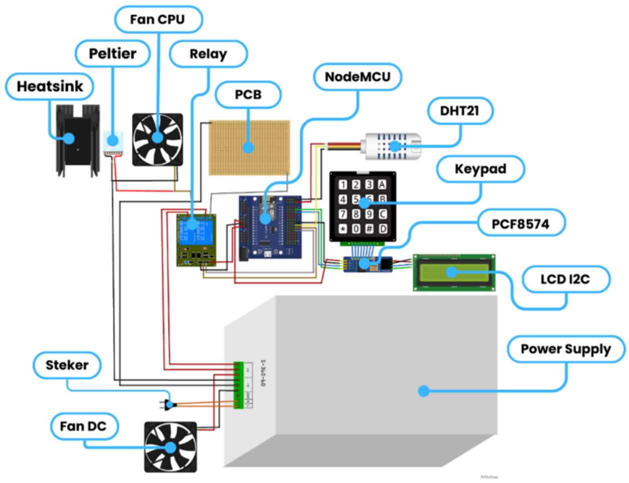

Figure 3. Hardware circuit

Table 2. Pin configuration of NodeMCU

Series	NodeMCU pins
PCF 8574	
SCL	D1
SDA	D2
GND	GND
VCC	VV
DHT11	
Inp	D5
GND	GND
VCC	3V
Relay	
VCC	VV
IN1	D5
IN2	D6
GND	GND

hardware, and control area as depicted in a schematic diagram as shown in Figure 2. Figure 3 shows a hardware circuit interconnecting the hardware components.

The pin configuration of the hardware circuit i.e. NodeMCU and power supply and relay (Figure 3) are tabulated in Table 2 and Table 3, respectively.

Table 3. Pin configuration of power supply and relay

Series	Power Supply	Relay
-	V+	L
-	V+	L
Cold Component		
Peltier +	-	Output1
Peltier -	V-	-
Fan CPU +	-	Output1
Fan CPU -	V-	-
Heat Component		
Positive	-	Output2
Negative	V-	-
Fan DC		
Positive	V+	-
Negative	V-	-
Steker		
L	L	-
N	N	-

The design of the ETC system consists of a main display (Figure 4) that contains a heat component in Figure 5a and a cold component in Figure 5b.

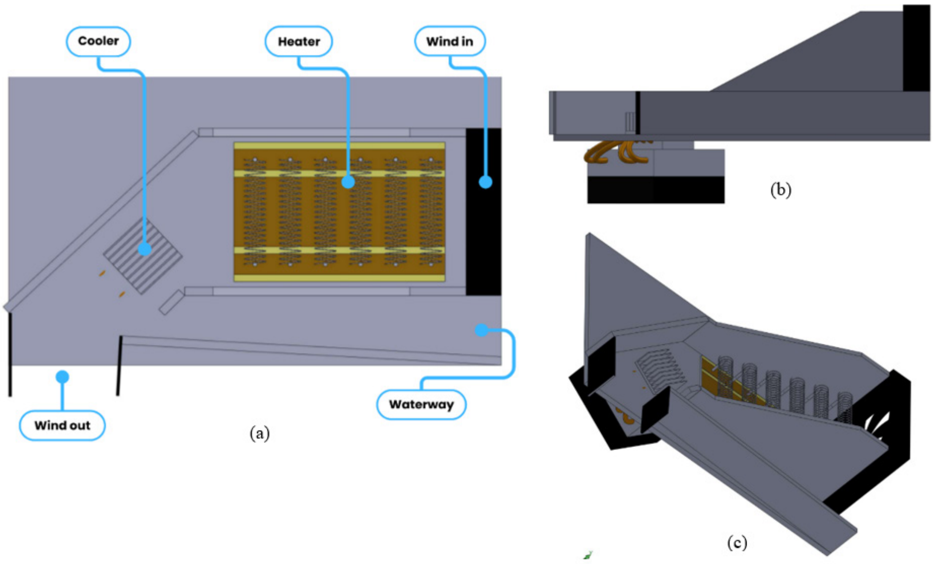

Figure 4. The design of the ETC system: (a) main view, (b) side view, and (c) corner view

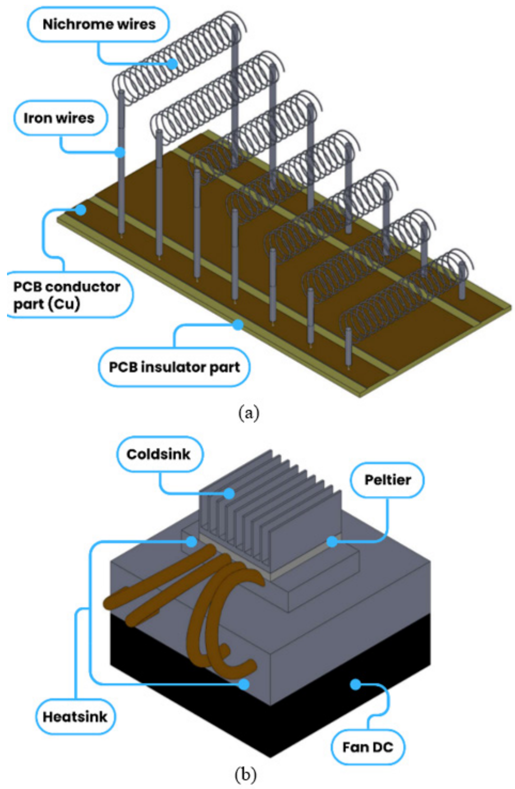

Figure 5. The component of ETC system (a) heat component, (b) cold component

The controller design is in the form of a box as shown in Figure 6. A monitoring system uses a I2C LCD and a controlling system uses a keypad.

C. Sensor Calibration

The DHT21 sensor is used as a temperature-measuring instrument. The calibration data of the DHT21 sensor is obtained by comparing the DHT21 sensor with a standardized temperature sensor (Elitech RC-4HC). Accuracy and precision analysis was carried out to validate the DHT21 sensor.

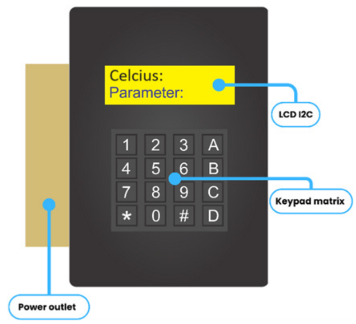

Figure 6. Controller design

Accuracy is the difference between the calculated value and actual values of a measurement. So that the measurement results can be said to be valid and objective. The error and accuracy of the DHT21 sensor can calculated using (1) and (2), respectively [25].

$$\%\text{Error} = \left| \frac{\overline{Y_n} - \overline{X_n}}{\overline{Y_n}} \right| \times 100\% \tag{1}$$

$$Accuracy = 100\% - \%Error. \tag{2}$$

Precision analysis is used to see the level of closeness of data from repeated measurements under the same conditions. Precision analysis is done by calculating the standard deviation (SD). SD is a precision instrument used to measure how each data point is grouped around the average [26]. The SD value is calculated as in the (3) [27].

$$\text{SD} = \sqrt{\frac{\sum_{i=1}^{N} \left(x_i - \overline{X}\right)^2}{N-1}} \tag{3}$$

where x_i is sensor reading results in the i-th experiment and N is the number of experiments.

Then, the precision results are reported in a manner such as (5) [26]:

$$\%\text{RSD} = \frac{\text{SD}}{\overline{X}} \times 100\% \tag{4}$$

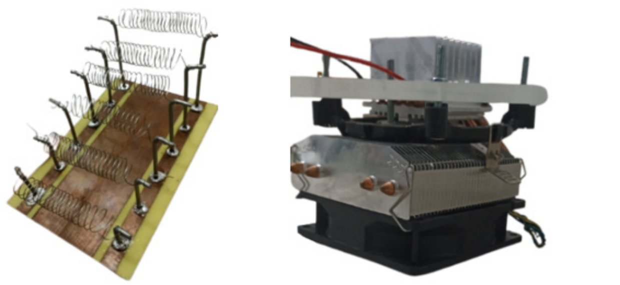

(a) (b)

Figure 7. The result of hardware design (a) heat component, (b) cold component

$$\text{Precission}_n = 100\% - \text{RSD}_n\,. \quad (5)$$

Relative standard deviation (RSD), also called coefficient of variation (CV), is a measure of dispersion that is relative (independent of the unit of measure used), so RSD can be used to compare the density of two groups. The RSD equation is used to convert the SD value into a percentage value. A good RSD value is ≤ 2% [26].

D. Performance Test

Testing the performance of the ETC system involves operating the system as a temperature regulator that can be adjusted to raise, maintain and lower the temperature. The DHT21 sensor was placed inside a semi-vacuum electrical spinning box in the test. Then, an Elitech RC-4HC was used to measure the temperature outside the box. A graph was then created showing the *x*-axis representing the DHT21 and the y-axis representing the Elitech RC-4HC.

III. Result and Discussion

A. Result of Hardware Design

The hardware has been finished, which includes the heat component (Figure 7a), the cold component (Figure 7(b)), the circuit ETC system (Figure 8a), the view of the ETC system (Figure 8b), and the controller box (Figure 8c).

The heat component is shown in Figure 7a, with nichrome wire as the main component to generate hot wind. The nichrome wire used is 24 American Wire Gauge (AWG), connected with two iron wires stuck on different printed circuit board (PCB) lines. While the cold component is shown in Figure 7b with Peltier as the main component to produce cold wind, the Peltier used has a voltage specification of 12 volts and a maximum current of 6 amperes. Peltier has a side that produces cold and the reverse side produces heat.

Figure 8 is the realization of the hardware, including Figure 8a, which depicts the circuit of ETC system, enclosed in a black box with dimensions of (11 X 7 X 18) cm^3 and equipped with a power outlet on the side. Figure 8b presents the primary display interface of the ETC system. Then Figure 8c shows the controller box with a keypad used to request the desired temperature and an

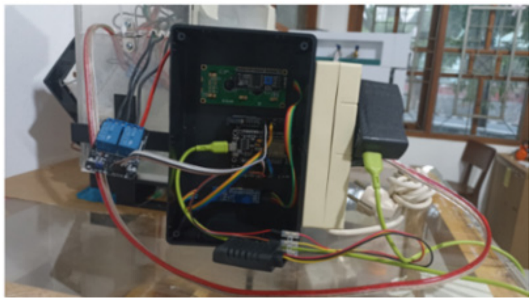

(a)

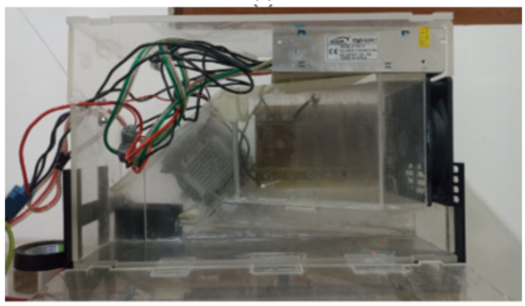

(b)

(c)

Figure 8. Overview of hardware design (a) the circuit of ETC system, (b) the front view of ETC system, (c) the controller box

LCD used to monitor the temperature of DHT21 placed in the electrospinning box.

B. Result of Software Design

The software has been finished, which includes the Blynk App (Figure 9) and Google Sheets. The Blynk display is set using features that can still be used freely, so it is shown in Figure 9 on the left there is a display of the temperature of the DHT21 that is read at that time, and on the right is a request for a temperature that can be set by swiping right or left.

Data temperature is stored in the cloud database to understand the dynamics of the temperature control process, facilitated by Google Sheets. The Google Sheets display shows column A as date data, column B as time data, column C as parameter data or the temperature to be targeted, column D as relay condition data, and column E as temperature data from the DHT21 sensor can be accessed using the following link: uns.id/GoogleSheetsLabfisDella.

C. Result of DHT21 Sensor Calibration

Testing the DHT21 sensor involves collecting calibration data for each sensor condition, comparing it

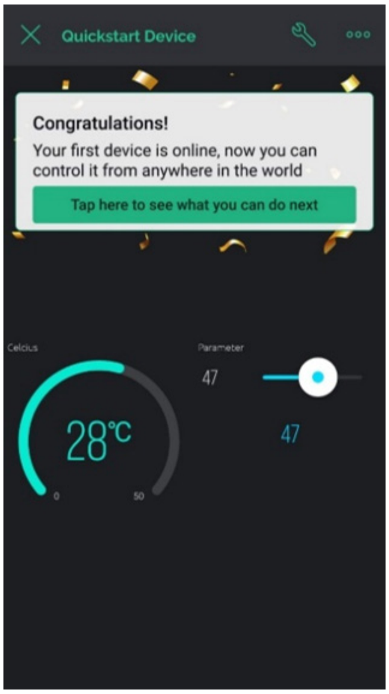

Figure 9. Result of Blynk App design

Table 4. . Data before calibration

No.	Temp (°C)	Elitech (°C)		DHT21 (°C)		RSD (%)	Preci-sion (%)	Er-ror (%)	Accu-racy (%)
		$\overline{X}$	SD	$\overline{X}$	SD				
1	0	0.62	0.06	-0.13	0.13	96.28	3.72	121	-21.00
2	10	10.75	0.13	9.69	0.20	2.09	97.91	9.86	90.14
3	20	20.30	0.07	19.61	0.07	0.38	99.62	3.40	96.60
4	30	30.68	0.10	30.28	0.13	0.43	99.57	1.30	98.70
5	40	40.57	0.32	40.07	0.29	0.73	99.27	1.23	98.77
6	50	50.11	0.17	49.72	0.20	0.40	99.60	0.78	99.22
7	60	60.33	0.31	60.23	0.18	0.29	99.71	0.17	99.83
8	70	70.52	0.20	70.37	0.31	0.44	99.56	0.21	99.79
9	80	80.30	0.31	80.37	0.24	0.30	99.70	0.09	99.91
		Average (%)				11.26	88.74	15.33	84.67

with the Elitech RC-4HC, and acquiring data as presented in Table 4.

Table 4 shows that the error obtained at a temperature of 0°C is 121%. This is because the difference between the temperature from DHT21 and Elitech at 0°C is 0.75°C, while the temperature from Elitech is 0.62°C, resulting in a %Error of 121%. This shows that the error value is 121% of the temperature value from Elitech.

Subsequently, the acquired data is processed to generate a graph to derive the linear regression equation. The data graph before calibration is illustrated in Figure 10.

The regression equation obtained from processing the graph is . Then, calibration is done by entering the regression formula into the coding uploaded using the Arduino IDE, as shown in Figure 11.

Once the successful upload is completed, the test is conducted again, and the data acquired post-calibration is displayed in Table 5.

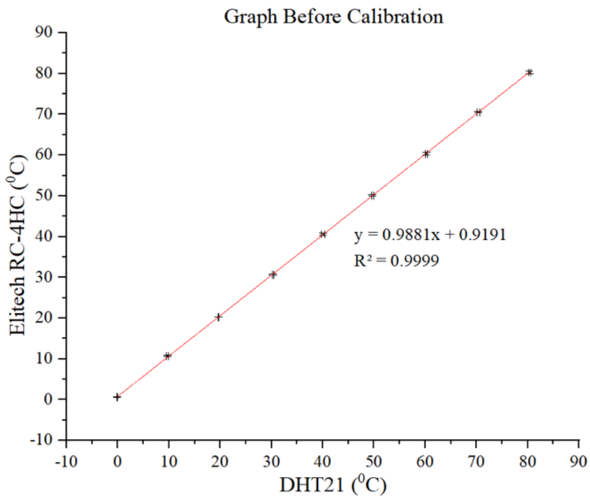

Figure 10. Graph comparing DHT21 with Elitech before calibration

```
Celcius = 0.9881*event.temperature+0.9191;
```

Figure 11. Display of entering regression formula in coding

Table 5. . Data after calibration

No.	Temp (°C)	Elitech (°C)		DHT21 (°C)		RSD (%)	Preci-sion (%)	Er-ror (%)	Accu-racy (%)
		$\overline{X}$	SD	$\overline{X}$	SD				
1	0	0.64	0.05	0.91	0.05	5.79	94.21	42.00	58.00
2	10	10.37	0.13	10.56	0.13	1.24	98.76	1.82	98.18
3	20	20.45	0.12	20.48	0.14	0.67	99.33	0.15	99.85
4	30	30.36	0.22	30.47	0.17	0.55	99.45	0.36	99.64
5	40	40.42	0.24	40.53	0.20	0.49	99.51	0.27	99.73
6	50	50.35	0.14	50.45	0.08	0.17	99.83	0.20	99.80
7	60	60.44	0.24	60.55	0.15	0.24	99.76	0.18	99.82
8	70	70.38	0.19	70.44	0.22	0.31	99.69	0.08	99.92
9	80	80.10	0.22	80.27	0.14	0.18	99.82	0.21	99.79
		Average (%)				1.18	98.93	5.05	94.95

After the calibration is obtained, the error value decreases from 15.33% to 5.05%, so the accuracy value increases from 84.67% to 94.95%. The RSD value decreased from 11.26% to 1.18%, so the precision value increased from 88.74% to 98.93%. The RSD value is smaller than 2%. Based on theory, a good RSD value is less than 2%, and the average RSD value obtained after calibration is 1.18%. Therefore, the data obtained has proven to be good.

After calibration, the data is processed in graphical form to determine the linear regression equation. The data graph after calibration is shown in Figure 12.

Based on Figure 12, the data processing results, the measurement result is $R^2 = 1$. This shows that the calibration results on DHT21 have a high level of linearity [28]. From the graph before and after calibration, it is found that the intercept data decreases from 0.9191 to 0.1713. The intercept value shows where a curve intersects the *y*-axis [29]. In addition, if the gradient value is close to 1, then the slope of the curve will be straight up, forming an angle of 45° to the *x*-axis [26]. Before and

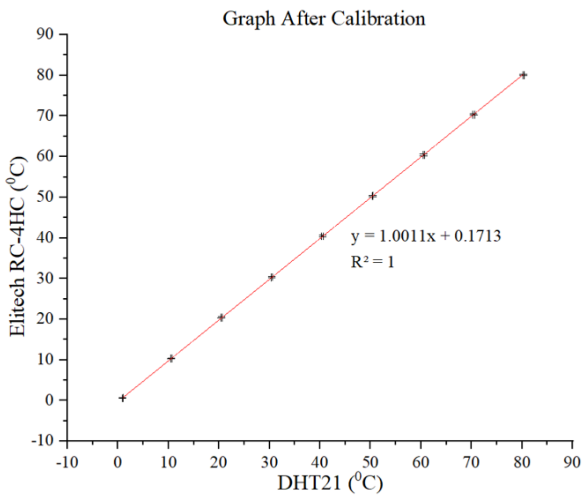

Figure 12. Graph comparing DHT21 with Elitech after calibration

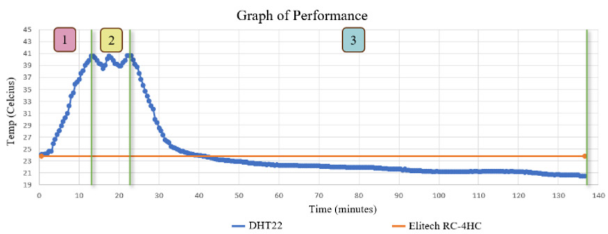

Figure 13. ETC system performance test chart

after calibration, the difference between the gradient and 1 decreases from 0.0119 to 0.0011. From the results of data and theory, it can be concluded that the curve has a high level of linearity, the intercept value is getting closer to 0, the gradient value is getting closer to 1, and the x value is getting closer to the y value.

D. Result of ETC System Performance

The ETC system test performance was carried out in several steps. The first step is the temperature is raised to 40°C, resulting in the heat component turning on for 13 minutes to raise the temperature from 24.04°C (initial temperature in the chamber) to 40°C (Condition 1). Next, the temperature is maintained at 40°C for 10 minutes, showing the heat and cold components turn on and off alternately (Condition 2). Next, the temperature is lowered to 20°C, which shows the cold component turning on (Condition 3). A graph displays time on the x-axis and temperature from DHT21 and Elitech on the y-axis, as shown in Figure 13.

Figure 13 proves that the performance of the ETC system is effective for raising the temperature but less effective for lowering the temperature. Although it can reduce about 3°C from the room temperature, the cooler still takes a long time.

E. Discussion

The results showed that the ETC system was successfully designed and built to regulate the temperature

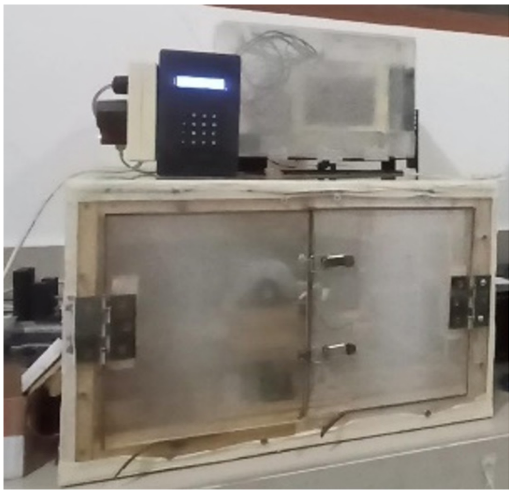

Figure 14. ETC system placement

inside the electrospinning box. This system is placed on top of a semi-vacuum box measuring (100 × 100 × 40) cm^3, as shown in Figure 14, and it can raise the temperature, maintaining temperature stability and lowering the temperature in the range of 20−40°C as shown in Figure 13. The ability of the ETC system to maintain a stable and controlled temperature can optimize the electrospinning process in producing nanofiber. This is in line with the research of G. Z Yang et al., 2017, which shows that the room temperature of the electrospinning box will affect the solvent evaporation rate [11].

In previous studies, the manufacture of temperature control for electrospinning has focused on heating the solution in the syringe pump [14], [15], [17]. At the same time, there is limited research on adjusting the room temperature, and few utilize cooling components. Therefore, the ETC system is set to flow hot or cold air according to the target temperature, as shown in Figure 4. The wind enters the ETC system through a heat component and a cold component, then is output through a funnel connected with the electrospinning box.

The controlling principle of the ETC system is divided into two types: close-range controlling by pressing the number on the keypad as the requested temperature (Figure 15) and remote controlling by sliding the temperature parameter on the display of the Blynk App available, as shown in Figure 16.

Besides remote control, IoT is also used to get cloud data using the Google Sheets platform. Every 30 seconds, data from the DHT21 sensor is sent to Google Sheets in real-time.

The ETC system has high accuracy in reading and regulating temperature, as evidenced by the calibration analysis of the DHT21 sensor which has an accuracy rate of 94.95% and a precision rate of 98.93%. These results indicate that the sensor reliably reflects actual temperature conditions and is well-suited for electrospinning.

Further performance testing reveals that the ETC system can operate within a 20−40°C temperature range, exceeding the optimal temperature range of 25−35°C

Figure 15. Close-range controlling

Figure 16. Remote controlling

typically recommended for the electrospinning process [12]–[14]. Despite this broader range, Figure 13 shows that the ETC system is effective for raising the temperature but less effective for lowering the temperature. Although it can reduce about 3°C from the room temperature, the cooler still takes a long time. This may be due to the improper treatment of the Peltier. Based on the paper Hebei I.T. (Shanghai) Co., when the Peltier is given a current of 1.5 A, the temperature difference between the two sides is around 20−30°C, therefore the more the hot side is cooled, the cool side will be cooler [30]. Hence, improvisation is needed to treat the hot side of the Peltier. Afshari investigated Peltier's heat management by comparing it with a water-cooling system and an air-cooling system, and it was found that water-cooling management was more effective [31]. Therefore, it is recommended to improve the cold component using water cooling for managing the Peltier hot side

IV. Conclusions

Based on the research, IoT-based electrospinning temperature control (ETC) system with a DHT21 sensor for controlling and monitoring temperature in an electrospinning box was successfully made. The DHT21 sensor has an accuracy rate of 94.95% and a precision rate of 98.93%. Three conditions are successfully applied to test the performance of the ETC system, including raising the temperature, maintaining temperature stability, and lowering the temperature. The ETC system performance data collection also proves that the system can control and monitor temperature. The ETC system is effective for raising the temperature but less effective for lowering the temperature, so it is recommended to improve the cold component using water cooling to manage the Peltier hot side.

Acknowledgment

The authors thank the E-SMART Research Group for providing laboratory facilities.

References

[1] O. M. Ikumapayi, E. T. Akinlabi, A. O. M. Adeoye, and S. O. Fatoba, "Microfabrication and nanotechnology in manufacturing system - An overview," *Mater. Today Proc.*, vol. 44, pp. 1154–1162, 2021.

[2] Q. Wu, W. S. Miao, Y. Du Zhang, H. J. Gao, and D. Hui, "Mechanical properties of nanomaterials: A review," *Nanotechnol. Rev.*, vol. 9, no. 1, pp. 259–273, 2020.

[3] S. N. Basahel, T. T. Ali, M. Mokhtar, and K. Narasimharao, "Influence of crystal structure of nanosized ZrO_2 on photocatalytic degradation of methyl orange," *Nanoscale Res. Lett.*, vol. 10, no. 1, 2015.

[4] D. Giljohann, D. Seferos, W. Daniel, M. Massich, P. Patel, and C. Mirkin, "Gold nanoparticles for biology and medicine," *Angew. Chem. Int. Ed. Engl.*, vol. 49, no. 19, pp. 3280–3294, 2014.

[5] Y. A. Rezeki, D. A. Hapidin, H. Rachmawati, M. M. Munir, and K. Khairurrijal, "Formation of electrosprayed composite nanoparticles from polyvinylpyrrolidone/mangosteen pericarp extract," *Adv. Powder Technol.*, vol. 31, no. 5, pp. 1811–1824, 2020.

[6] Y. Gao, Y. B. Truong, Y. Zhu, and I. Louis Kyratzis, "Electrospun antibacterial nanofibers: Production, activity, and in vivo applications," *J. Appl. Polym. Sci.*, vol. 131, no. 18, pp. 9041–9053, 2014.

[7] A. V., S. R., G. Angadi, and N. M. H.N., "A comprehensive review summarizing the effect of electrospinning parameters and potential applications of nanofibers," *J. Nanosci. Nanoeng. Appl.*, vol. 9, no. 3, pp. 1–6, 2019.

[8] S. M. Tan *et al.*, "Electrospinning and its potential in fabricating pharmaceutical dosage form," *J. Drug Deliv. Sci. Technol.*, vol. 76, p. 103761, Oct. 2022.

[9] A. Luraghi, F. Peri, and L. Moroni, "Electrospinning for drug delivery applications: A review," *J. Control. Release*, vol. 334, pp. 463–484, 2021.

[10] Q. Zhang *et al.*, "Temperature-controlled reversible pore size change of electrospun fibrous shape-memory polymer actuator based meshes," *Smart Mater. Struct.*, vol. 28, no. 5, pp. 22–24, 2019.

[11] G. Z. Yang, H.-P. Li, J.-H. Yang, J. Wan, and D.-G. Yu, "Influence of working temperature on the formation of electrospun polymer nanofibers," *Nanoscale Res. Lett.*, vol. 12, pp. 1–10, 2017.

[12] F. Huang, Q. Wei, J. Wang, Y. Cai, and Y. Huang, "Effect of temperature on structure, morphology and crystallinity of PVDF nanofibers via electrospinning," *E-Polymers*, no. 152, pp. 1–8, 2008.

[13] O. Hardick, B. Stevens, and D. G. Bracewell, "Nanofibre fabrication in a temperature and humidity controlled environment for improved fibre consistency," *J. Mater. Sci.*, vol. 46, pp. 3890–3898, 2011.

[14] D. Thuy *et al.*, "Temperature effects on electrospun chitosan nanofibers," *Green Process. Synth.*, vol. 9, pp. 488–495, 2020.

[15] H. M. Chen and D. G. Yu, "An elevated temperature electrospinning process for preparing acyclovir-loaded PAN ultrafine fibers," *J. Mater. Process. Technol.*, vol. 210, no. 12, pp. 1551–1555, 2010.

[16] H. Lara-Padilla, C. Mendoza-Buenrostro, D. Cardenas, A. Rodriguez-Garcia, and C. A. Rodriguez, "Influence of controlled cooling in bimodal scaffold fabrication using polymers with different melting temperatures," *Materials (Basel).*, vol. 10, no. 6, pp. 1–16, 2017.

[17] D. Abbas, M. S. Mu'min, M. Bonanno, S. Thiele, and T. Böhm, "Active solution heating and cooling in electrospinning enabling spinnability from various solvents," *J. Appl. Polym. Sci.*, vol. 139, no. 31, pp. 1–11, 2022.

[18] J. Lv, Q. Zhou, P. Chen, Y. Wang, and W. Wang, "Effect of receiver plate temperature and magnetic lens on the performance of electrospun PAN," *Colloids Surfaces A Physicochem. Eng. Asp.*, vol. 676, no. PA, p. 132130, 2023.

[19] A. V. Midyk and O. Lysa, "Studies of temperature-humidity characteristics of the greenhouse cyber-physical system," *Вимірювальна техніка та метрологія*, no. 2, pp. 7–12, 2020.

[20] S. Dubey, M. C. Chinnaiah, I. A. Pasha, K. Sai Prasanna, V. Praveen Kumar, and R. Abhilash, "An IoT based Ayurvedic approach for real time healthcare monitoring," *AIMS Electron. Electr. Eng.*, vol. 6, no. 3, pp. 329–344, 2022.

[21] Aosong, *Temperature and humidity module AM2301 Product Manual*. 2017. [Online]. Available: www.aosong.com

[22] H. Durani, M. Sheth, M. Vaghasia, and S. Kotech, "Smart automated home application using IoT with Blynk App," in *2018 Second international conference on inventive communication and computational technologies (ICICCT)*, 2018, pp. 393–397.

[23] I. Plauska, A. Liutkevičius, and A. Janavičiūtė, "Performance evaluation of C/C++, micropython, rust and tinygo programming languages on ESP32 microcontroller," *Electronics*, vol. 12, no. 1, p. 143, 2022.

[24] D. Firdaus, "Permainan disco TKO menggunakan Google Sheets sebagai upaya meningkatkan kualitas pembelajaran matematika pada siswa kelas IXA SMP Negeri 1 Welahan," *J. Pendidik. Indones.*, vol. 3, no. 02, pp. 153–160, 2022.

[25] S. W. Suciyati, M. S. Hidayatullah, and G. A. Pauzi, "An analysis of data acquisition system of temperature, oxygen, and carbon dioxide in refrigerator with Arduino Mega 2560," *J. Ilm. Pendidik. Fis. Al-Biruni*, vol. 10, no. 1, pp. 119–127, 2021.

[26] A. Setyawan, "Validasi metoda analisis besi (Fe) pada limbah radioaktif cair menggunakan spektrofotometer serapan atom berdasarkan SNI 6989.4:2009 dan SOP-PTLR," in *Prosiding Hasil Penelitian dan Kegiatan*, 2018, pp. 93-102. Pusat Teknologi Limbah Radioaktif-BATAN.

[27] D. K. Lee, J. In, and S. Lee, "Standard deviation and standard error of the mean," *Korean J. Anesthesiol.*, vol. 68, no. 3, pp. 220–223, 2015.

[28] D. Kurnia, "Analisis signifikansi Leverage dan kebijakan deviden terhadap nilai perusahaan," *J. Account.*, vol. 4, no. 2, pp. 12–21, 2017.

[29] N. Pandis, "Linear regression," *Am. J. Orthod. Dentofac. Orthop.*, vol. 149, no. 3, pp. 431–434, 2016.

[30] L. Hebei I.T. (Shanghai) Co., "Performance specifications of TEC1-12706," *Appl. Note*, pp. 2–4, 2010, [Online]. Available: www.hebeiltd.com.cn

[31] F. Afshari, "Experimental and numerical investigation on thermoelectric coolers for comparing air-to-water to air-to-air refrigerators," *J. Therm. Anal. Calorim.*, vol. 144, no. 3, pp. 855–868, 2020.